Original Research

Strength Characteristics and Mechanism of CMK Cement Soil in a Na_2SO_4 Solution Environment

Jianping Liu[1, 2], Jianjun Xu[1], Guoshuai Xie[1], Xiangqian Xie[1], Jixia Zhang[1], Xiaohong Bai[3, 4] *

[1]Engineering Test Center, PowerChina Huadong Engineering Corporation Limited, Hangzhou 310014, China
[2]College of Civil Engineering and Architecture, Zhejiang University, Hangzhou 310058, China
[3]College of Civil Engineering, Taiyuan University of Technology, Taiyuan 030024, China
[4]Key Laboratory of Geotechnical and Underground Engineering of Shanxi Province, Taiyuan 030024, China

Abstract

Coal-bearing metakaolin (CMK) is a highly active volcanic material. In this study, the compressive strength of CMK cement soil was tested, along with five CMK samples cured in different concentrations of Na_2SO_4 solution. The compressive strength of the CMK cement soil first increased and then decreased with increasing Na_2SO_4 concentrations. When the Na_2SO_4 solution concentration was 18 g/L, the compressive strength of the CMK cement soil reached its maximum value. Additionally, X-ray diffraction (XRD) analysis of the chemical reactions between the CMK cement soil and Na_2SO_4 solution and scanning electron microscopy (SEM) were used to analyze the phase composition and microstructure of the CMK cement soil, respectively. Thus, the pore distribution of the CMK cement soil could be calculated and classified from a 500× magnification SEM image using Image-ProPlus6.0 analysis software. This study explains the mechanism of curing CMK cement soil in a Na_2SO_4 solution based on its phase analysis, microstructure, and pore distribution.

Keywords: CMK cement soil, sodium sulfate solution, compressive strength, phase analysis, microstructure

Introduction

Cement soil is an artificial mixed material formed by stirring natural soft soil and cement slurry (or powder) via mechanical stirring or jet punching processes [1, 2]. It is primarily a mixture of cement and soil [3, 4]. Because of its low price, wide material availability, simple construction process, and excellent performance, cement soil is widely used in foundation treatments and roadbed engineering [5, 6]. In practical engineering, groundwater is often polluted by acidic and alkaline pollutants, the pH of which can have a significant impact on the strength characteristics of cement soil [7, 8]. Additionally, the erosion of cement soil in a sulfate environment is also significant [9, 10]. Bai et al. (2007) compared and analyzed the stress-strain curve of cement soil in clear water and a chemical solution environment using indoor simulation experiments and established the relationship between the compressive strength and erosion time [11]. Dong et al. (2011) tested the strength

of cement-solidified sodium-sulfate-contaminated soil of different content through laboratory simulation experiments and discovered the relationship between the resistivity and compressive strength of contaminated cement soil [12]. Liu et al. (2014) simulated a seawater erosion environment using different concentrations of sodium chloride, magnesium chloride, and magnesium sulfate solutions and evaluated the effects of the solution concentration on the unconfined compressive strength and microstructure of cement soil [13]. Chen et al. (2016) studied the influence of corrosive medium environment on the mechanical properties of cement soil and found that trace sodium sulfate corrosion solution was conducive to its hydration and compaction [14]. Kampala et al. (2021) analyzed the influence of a sulfate medium on the compaction characteristics and strength development of cement soil and derived a curve for the relationship between the unconfined compressive strength and optimum moisture content [15]. These studies aside, there have been few studies on the compressive strength of cement soils containing additives in corrosive environments.

Metakaolin (MK) is an anhydrous calcium aluminate ($Al_2O_3 \cdot 2SiO_2$, AS_2) formed by the calcination and dehydration of kaolin ($Al_2O_3 \cdot 2SiO_2 \cdot 2H_2O$, AS_2H_2) at a certain temperature (500ºC~900ºC) [16, 17]. Coal-bearing metakaolin (CMK) – composed of active silica and alumina – is produced via the calcination of coal kaolin [18, 19]. Recently, MK has been widely used to improve the mechanical properties, impermeability, and durability of cement-based materials [20-23]. Siddique et al. (2009) summarized the research progress on MK in concrete, the results of which showed that MK could improve the corrosion resistance of concrete [24]. Janotka et al. (2010) studied the influence of low-grade MK on the strength of cement mortar and found that it could improve its strength and impermeability [25]. Hassan et al. (2012) evaluated the effect of MK on the rheology of concrete and found that the plastic viscosity and yield strength of concrete were positively correlated

with the MK content [26]. Deng et al. (2016) partially replaced cement with MK in cement soil and found that MK greatly enhanced its penetration resistance [27]. Wang et al. (2022) discussed the effects of MK on the permeability characteristics of cemented silty sand and determined the relationship between the permeability coefficient and unconfined compressive strength [28].

Nonetheless, in general, there have been few studies on the impact of CMK incorporation into cement soil, particularly on its durability. In this study, the compressive strength of CMK cement soil was studied using laboratory simulation experiments, along with five CMK samples cured in different concentrations of sodium sulfate (Na_2SO_4) solution. X-ray diffraction (XRD) technology was used to analyze the chemical reactions of Na^+ and SO_4^{2-} in the CMK cement soil and scanning electron microscopy (SEM) technology was used to determine its microstructure. The average pore size was calculated from the 500× magnification SEM image using Image-ProPlus6.0 analysis software and the mechanism of CMK cement soil curing in a Na_2SO_4 environment was discussed.

Materials and Methods

Experimental Materials

The soil was collected from a construction site in Taiyuan, Shanxi Province, China. The soil particles were passed through a 2.0 mm sieve. Table 1 lists the particle-size distributions. The coefficients of uniformity (C_u) and curvature (C_c) are 0.76 and 3.65, respectively, which is poorly graded sandy soil according to the Chinese GB50021-2001 standard [29]. The ordinary Portland cement (OPC) was produced in Taiyuan, China. The 28 d compressive strength of the cement is 42.5 MPa, and the particle size distribution range is 5 μm~10 μm. Table 2 lists the chemical composition of the cement. The CMK was obtained from Shanxi Bright

Table 1. Particle size distribution of sandy soil.

Particle size /mm	2.00~0.50	0.50~0.25	0.25~0.075	0.075~0.005	<0.005
Content /wt.%	18.0	25.0	21.0	24.0	12.0

Table 2. Chemical composition of cement.

Oxides	SiO_2	Al_2O_3	Fe_2O_3	CaO	MgO	K_2O	Na_2O	SO_3	Other
Content /%	18.81	5.86	3.34	66.35	1.04	0.41	0.31	2.53	1.35

Table 3. Chemical composition of CMK.

Oxides	SiO_2	Al_2O_3	Fe_2O_3	TiO_2	CaO	MgO	K_2O	Na_2O
Content /%	52.62	45.42	0.45	0.85	0.17	0.11	0.13	0.25

Table 4. Mix proportions for the preparation of CMK cement soil samples.

Sample	Sandy soil content /%	CMK content /%	Cement content /%	Water consumption /%
CMK0	100	0	15	20
CMK1	100	2	13	20
CMK2	100	3	12	20
CMK3	100	4	11	20
CMK4	100	5	10	20

Note: The CMK content, cement content and water consumption are the percentage of the required water mass in the total mass of sandy soil.

Kaolin Technology Co., Ltd., China. Particles smaller than 2 μm account for more than 90% of the total mas. Table 3 lists the chemical composition of the CMK. The sodium sulfate reagent was analytically pure anhydrous Na_2SO_4 with a purity of more than 99%, produced by the Tianjin Reagent Factory Co., Ltd., China. The pH of the Na_2SO_4 reagent was maintained between 5 and 8 at room temperature.

Sample Preparations

Prior to sample preparation, sandy soil was dried in an oven at 105ºC for 24 h. Table 4 lists the mix proportions for the preparation of the CMK cement soil. During the sample preparation, the sandy soil, CMK, cement, and distilled water were weighed, as listed in Table 4. All mixtures were poured into a mixer for two min to ensure uniform stirring of the slurry. The slurry was then added in two steps to a 70.7 mm × 70.7 mm × 70.7 mm steel mold. After adding one-third of the slurry, the steel mold was vibrated on a vibration table for one min to ensure that all air was exhausted. The sample surface was scraped flat using a scraper, and the steel mold was wrapped in plastic. After 24 h, the mold was removed. The samples were cured in a constant-temperature water tank for 7 d. Finally, all the CMK cement-soil samples were removed and placed in solutions of different Na_2SO_4 concentrations to continue curing for 28 d. The concentrations of the Na_2SO_4 solutions were 0, 4.5 g/L, 9 g/L, 18 g/L and 36 g/L, respectively, according to the Chinese GB50021-2001 standard [29]. The samples in the five different environments were denoted as NS0, NS1, NS2, NS3, and NS4.

Testing Methods

The compressive strengths of the CMK cement-soil samples at 28 d were tested using a WDW-100 electronic universal testing machine at a loading rate of 0.3 kN/s. Phase composition tests of the CMK cement-soil samples were performed at 28 d using a Shimadzu Suzhou XRD-6000 X-ray diffractometer, the scanning angle ranging from 2°~60° and the speed being 6°/min. Microscopic images of the CMK cement-soil samples at 28 d were captured using a Hitachi TM-3000 scanning

electron microscope, at magnifications of 500× and 5000×.

After the test, the XRD peaks were analyzed using MDI Jade 6.0 software, to determine the phase composition of the CMK cement soil. Additionally, Image-ProPlus6.0 analysis software was used to process and analyze the SEM images at 500× magnification to obtain the pore distribution of the CMK cement soil.

Results and Discussion

Compressive Strength

Fig. 1 shows the compressive strength of the CMK cement soil cured in different Na_2SO_4 solution concentrations at 28 d. In general, compared with the CMK cement soil cured in clear water (Na_2SO_4 concentration of 0), the compressive strength of the CMK cement soil increases to differing degrees with increasing Na_2SO_4 solution concentration. When the Na_2SO_4 solution concentration is less than 18 g/L, the compressive strength of the CMK cement soil increases with increasing Na_2SO_4 solution concentration. When the Na_2SO_4 concentration is greater than 18 g/L, the compressive strength of the CMK cement soil decreases with increasing Na_2SO_4 solution concentration. Within the scope of the experiment designed in this study, when the Na_2SO_4 solution concentration is 18 g/L, the strength of the CMK cement soil reaches its maximum value, indicating that a moderate Na_2SO_4 solution concentration has a crucial enhancing effect on the CMK cement soil strength. It should be noted that the relationship between the compressive strength of the CMK cement soil and the CMK content has been previously reported [30, 31]. When the CMK content is 3%, the strength of the CMK cement soil reaches its maximum value. Consequently, the CMK cement soil with 3% CMK content cured in different concentrations of Na_2SO_4 solution was selected for microscopic analysis.

XRD Analysis

Fig. 2 shows the XRD patterns of the CMK cement soil with 3% CMK content cured in different
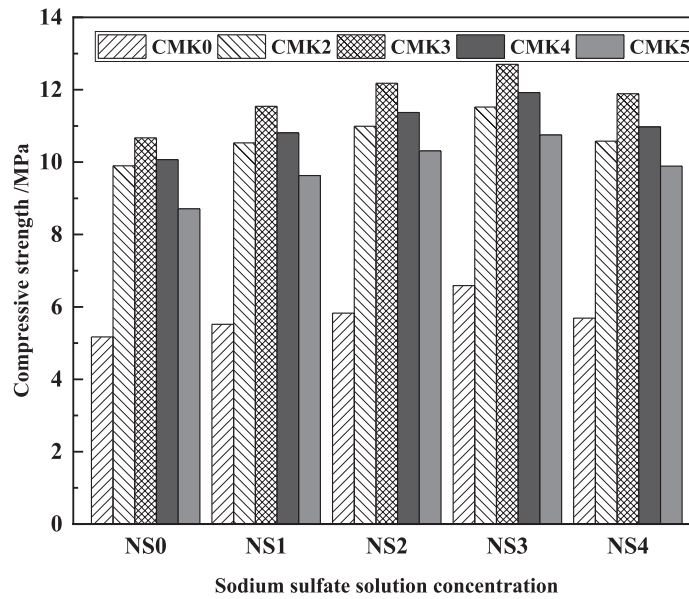
Fig. 1. Compressive strength of CMK cement soil at 28d in the Na_2SO_4 solution environment.
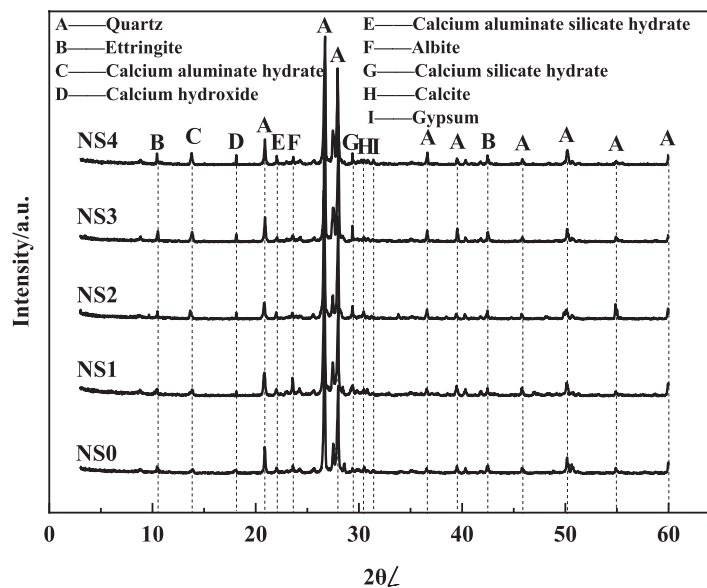
Fig. 2. XRD patterns of CMK cement soil at 28d in the Na_2SO_4 solution environment.

concentrations of Na_2SO_4 solution at 28 d. The main phases of the CMK cement soil are quartz, ettringite, calcium aluminate hydrate, calcium hydroxide, calcium aluminate silicate hydrate, albite, calcium silicate hydrate, calcite, and gypsum. The CMK cement soil is reinforced mainly through the hydrolysis and hydration of MK and cement, the interaction between the soil particles and hydration products, and carbonation [32]. Moreover, the interaction between the soil particles and hydration products manifests as an ion-exchange agglomeration reaction and a pozzolanic reaction. Additionally, Na^+ and SO_4^{2-} participate in chemical reactions in the CMK cement soil. The chemical reactions between Na^+ and the CMK cement soil can be expressed as follows [33]:

$$Ca(OH)_2 + Na_2SO_4 \cdot 10H_2O = CaSO_4 \cdot 2H_2O \cdot 2NaOH + 8H_2O$$

$$3CaO \cdot 2SiO_2 \cdot 3H_2O + 4NaOH = 3Ca(OH)_2 + 2Na_2SiO_3 + 2H_2O$$

$$3CaO \cdot Al_2O_3 \cdot 6H_2O + 2NaOH = 3Ca(OH)_2 + Na_2O \cdot Al_2O_3 + 4H_2O$$

$$Na_2O \cdot Al_2O_3 + 6SiO_2 = Na_2O \cdot Al_2O_3 \cdot 6SiO_2$$
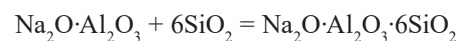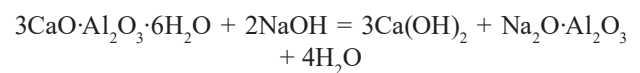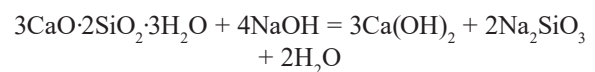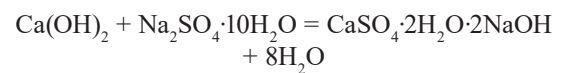
The reaction equation shows that calcium hydroxide $(Ca(OH)_2)$ is the product of the Na^+ reaction. As shown in Fig. 2, the peak value of calcium hydroxide increases as the reaction progresses – that is, as the Na_2SO_4 solution

concentration increases, more calcium hydroxide is produced. Moreover, the hydration reactions of cement produce large quantities of calcium hydroxide [34].

As shown in Fig. 1, when the Na_2SO_4 solution concentration is less than 18 g/L, the compressive strength of the CMK cement soil increases with increasing Na_2SO_4 solution concentration. This is because the production of calcium hydroxide continues to improve the overall CMK cement-soil strength in three ways: First, $Na_2O \cdot Al_2O_3$ reacts chemically with SiO_2 to produce albite ($Na_2O \cdot Al_2O_3 \cdot 6SiO_2$) owing to the presence of Na^+. Moreover, Na^+ has a larger ionic radius in albite, which can cause an ion exchange with Ca^{2+} in the calcium hydroxide [35]. All calcium hydroxides are produced by the hydration of cement and CMK, as well as by the reaction between Na^+ and the cement soil. After ion exchange, the diffusion layer of the electric double layer in the cement-soil system weakens. Consequently, the volume of bound water is reduced, thereby increasing the direct cohesion of soil particles and improving the strength of the soil [36]. Additionally, the generated Ca^{2+} chemically reacts with active SiO_2 and Al_2O_3 in the sandy soil and CMK to produce calcium silicate hydrate ($3CaO \cdot 2SiO_2 \cdot 3H_2O$) and other products in alkaline environments [37]. These hydration products bond with the soil particles to form a cemented network structure, which continues to increase the strength of the cement soil. Finally, part of the free calcium hydroxide is carbonized with carbon dioxide in air and water to produce calcite ($CaCO_3$), which also enhances the strength of the cement soil [38].

The chemical reactions between SO_4^{2-} and CMK cement soil can be expressed as follows [39]:

$$CaSO_4 + 2H_2O = CaSO_4 \cdot 2H_2O$$

$$3CaSO_4 + 4CaO \cdot Al_2O_3 \cdot 19H_2O + 14H_2O$$
$$= 3CaO \cdot Al_2O_3 \cdot 3CaSO_4 \cdot 32H_2O + Ca(OH)_2$$

$$3CaSO_4 \cdot 3CaO \cdot Al_2O_3 \cdot CaSO_4 \cdot 18H_2O + 14H_2O$$
$$= 3CaO \cdot Al_2O_3 \cdot 3CaSO_4 \cdot 32H_2O$$
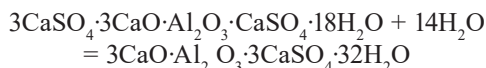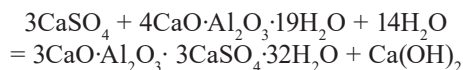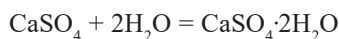
Here, $SO4^{2-}$ reacts with the cement soil to form gypsum ($CaSO_4 \cdot 2H_2O$), which has an expansion effect on the cement soil [40]. Additionally, gypsum reacts with calcium aluminate hydrate ($4CaO \cdot Al_2O_3 \cdot 19H_2O$) and monosulfur calcium aluminate hydrate ($3CaO \cdot Al_2O_3 \cdot CaSO_4 \cdot 18H_2O$) to form ettringite ($3CaO \cdot Al_2O_3 \cdot 3CaSO_4 \cdot 32H_2O$). Ettringite is characterized primarily by its filling and expansion effects [41]. When the generation of ettringite is low during the early stages, the space network structure formed by the intersecting ettringite crystals and calcium silicate hydrate fills the gaps in the cement-soil particles. This reduces the porosity and increases the strength. However, during the later stages, with an increase in the number of ettringites, the expansion effect is not conducive to cementation between the soil particles, contributing to a decrease in the cement-soil strength.

As shown in Fig. 1, when the Na_2SO_4 solution concentration is greater than 18 g/L, the compressive strength of the CMK cement soil decreases with increasing Na_2SO_4 solution concentration. This is because large quantities of Na^+ and SO_4^{2-} participate in the reaction. Sodium hydroxide (NaOH) undergoes a chemical reaction with the calcium silicate hydrate produced by the hydration of cement and CMK, leading to poor cementation between the soil particles. This is reflected in the reduction in the cement-soil strength. Furthermore, the gypsum and ettringite generated by excessive SO_4^{2-} exhibit expansion effects, generating a large swelling force. This increases the volume of the soil particles and damages its internal structure, causing a reduction in the cement-soil strength.

SEM Analysis

Fig. 3 shows SEM images of the CMK cement soil with 3% CMK content cured in different concentrations of Na_2SO_4 solution at 28 d. As shown in Fig. 3a), the soil particles of the CMK cement samples cured in clean water are bonded through flocculent cementitious products. However, some pores remain between soil particles. The strength of the flocculent cementitious products is low, and they are relatively loosely arranged. Once the soil particles are disturbed by external forces, their internal microstructures can be easily destroyed.

Fig. 3(b-d) shows SEM images of the CMK cement-soil samples cured in different concentrations of Na_2SO_4 solutions. When the Na_2SO_4 solution concentration is less than 18g/L, more and more flocculent cementitious products are generated from the hydration reaction of the CMK cement soil with increasing Na_2SO_4 solution concentration. This flocculent cementitious product wraps the soil particles from all sides, promoting firmer soil particles. With increasing Na_2SO_4 solution concentration, an increasing number of needle-shaped and rod-shaped ettringites are generated by the hydration reaction of the cement soil. The pores between the soil particles are effectively filled with ettringite, thereby reducing the number of pores. The structural units of the soil particles are granulated to ensure that the soil structure is stable.

As shown in Fig. 3e), when the Na_2SO_4 solution concentration exceeds 18 g/L and reaches 36 g/L, a large quantity of ettringite crystals are generated during the hydration reaction of the CMK cement soil. In addition to filling the pores between the soil particles, these ettringite crystals are attached to the surface of the soil particles, forming a part of the acicular soil particle structure. Because of the expansion effect produced by ettringite crystals, the volume of the CMK cement soil expands rapidly, and the pores become larger. When the expansion effect produced by ettringite is greater than the cementation effect between the soil particles, the soil is damaged, leading to a decrease in the cement-soil strength [42].

a) NS0

b) NS1

c) NS2

d) NS3

e) NS4
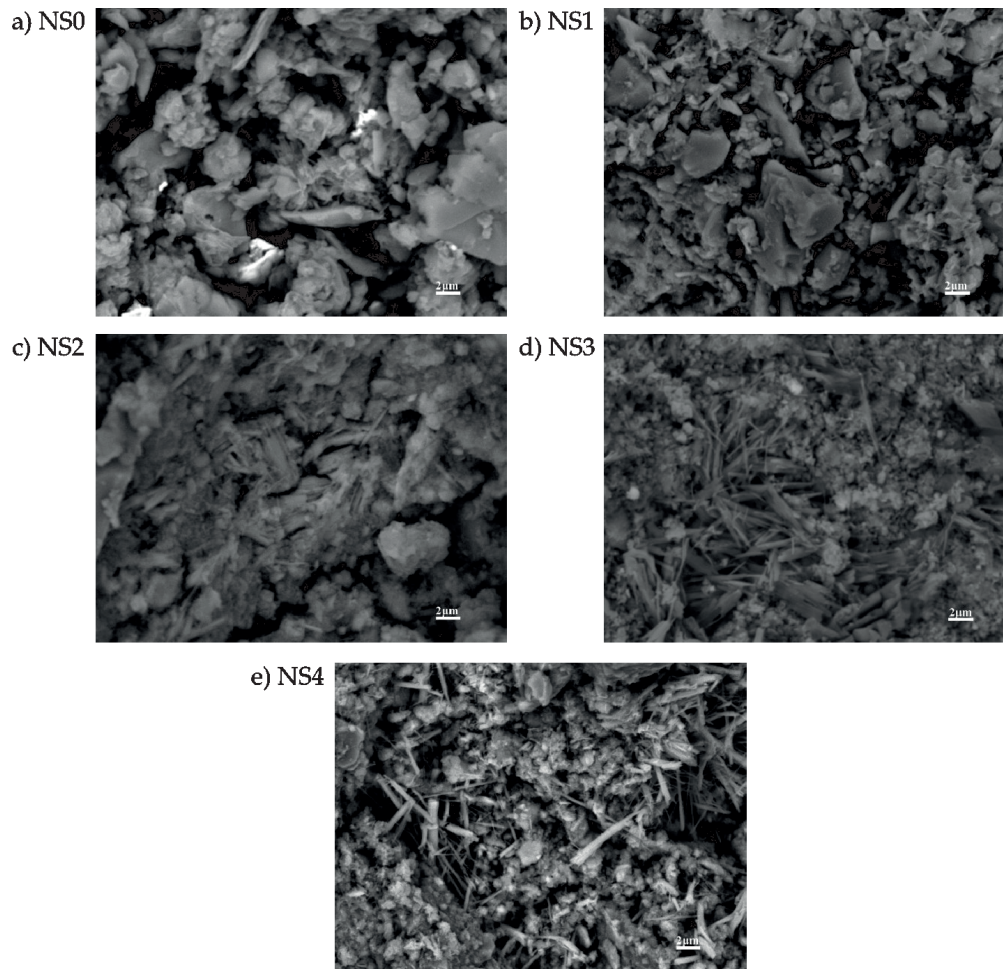
Fig. 3. SEM images at 5000× magnification of CMK cement soil at 28d in the Na_2SO_4 solution environment.

Pore Distribution Analysis

To obtain the pore distribution of CMK cement soil cured in different concentrations of Na_2SO_4 solution, SEM images of the CMK cement soil at 500× magnification were processed using Image-ProPlus 6.0 analysis software. Fig. 5 shows the original SEM images and binary images of the CMK cement soil with 3% CMK content cured in different concentrations of Na_2SO_4 solution at 28 d. The size of the pores was calculated using the black and white binarized images, the classification and statistical parameters of which are listed in Table 5.

From the statistical results of the sample porosity in Table 5, the porosity of the CMK cement soil in Na_2SO_4 solution is considerably lower than that in clean water. Moreover, with an increase in the Na_2SO_4 solution concentration, the porosity first decreases before increasing. When the concentration of the Na_2SO_4 solution is 18 g/L, the porosity reaches its minimum value of 26.52%. This is because the hydration products generated by the reaction between the CMK cement soil and Na_2SO_4 solution play a far greater role in filling than the hydration products generated by the CMK cement soil. Consequently, the CMK cement-soil

porosity decreases, and the CMK cement-soil strength increases in the Na_2SO_4 solution. When the Na_2SO_4 solution concentration is too high, the gypsum and ettringite generated by the CMK cement soil and Na_2SO_4 solution contributes to the expansion. Consequently, the porosity of the CMK cement soil increases and the CMK cement-soil strength decreases in the Na_2SO_4 solution [43].

Based on the size of the average pore diameter, the microscopic pores of the sample can be divided into the following five categories – that is, micro pores (<2 μm), small pores (2 μm~5 μm), medium pores (5 μm~20 μm), macro pores (20 μm~50 μm), and holes (>50 μm) [44, 45]. From the statistical analysis of the pore distribution shown in Table 5, it is evident that the pore distribution of the CMK cement soil changes owing to the influence of the Na_2SO_4 solution. The distribution proportions of micro pores, small pores, and medium pores all initially increase before decreasing with increasing Na_2SO_4 solution concentration – that is, the proportion of all the pores in sample NS3 reaches its maximum. By contrast, the distribution proportion of macro pores first decreases before increasing with increasing Na_2SO_4 solution concentration – that is, the proportion of NS3 reaches its minimum value. Moreover,

a) NS0

b) NS1

c) NS2

d) NS3

e) NS4
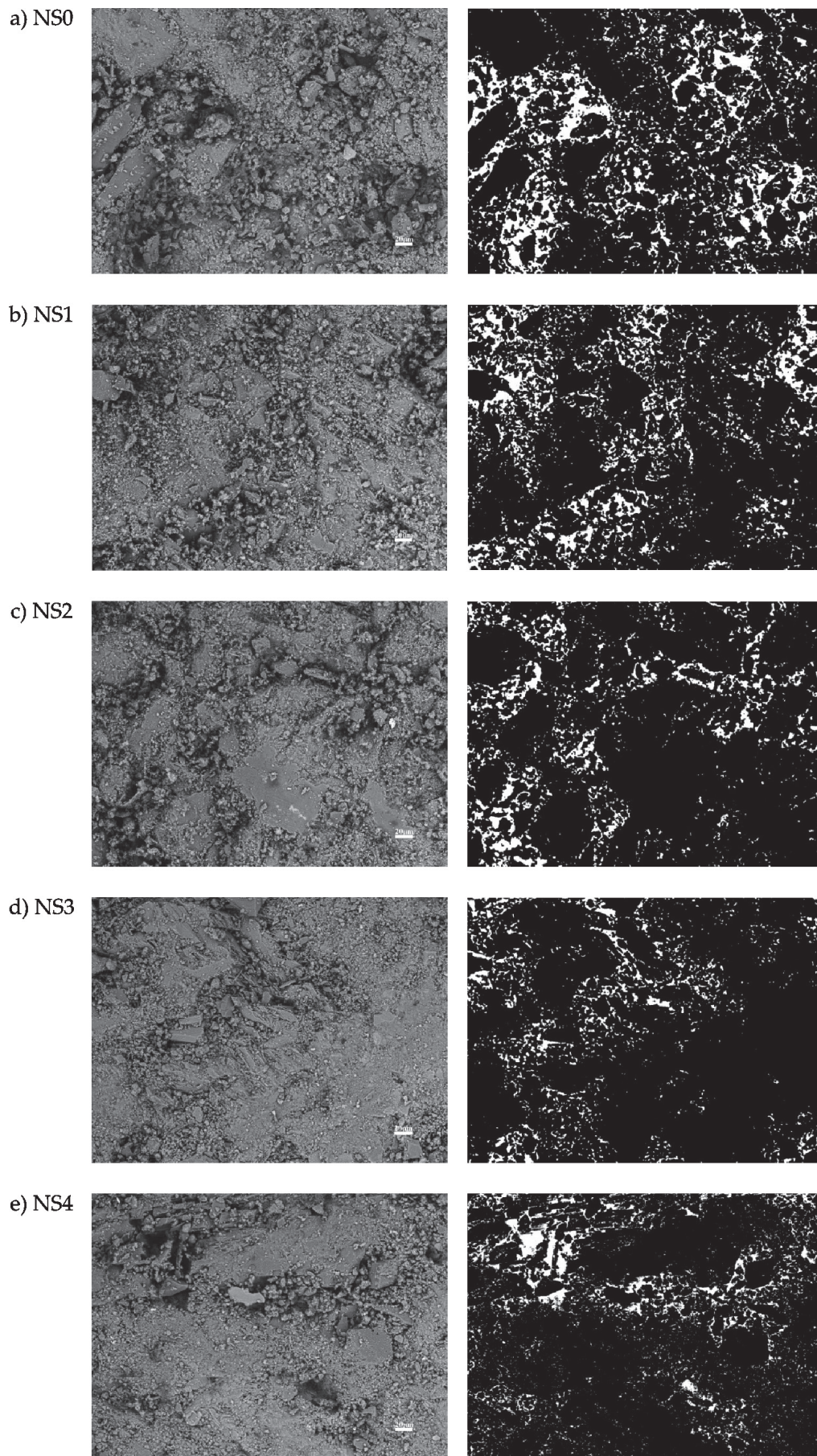
Fig. 4. Original SEM images and binarized images at 500×magnification processed by Image-ProPlus6.0 analysis software of CMK cement soil at 28d.

Table 5. Mix proportions for the preparation of CMK cement soil samples.

Sample	Percentage of various pore areas in the total pore area /%					Porosity /%
	<2 μm	2 μm~5 μm	5 μm~20 μm	20 μm~50 μm	>50 μm	
NS0	3.32	29.96	30.23	31.85	27.22	29.96
NS1	3.55	28.73	37.35	27.81	23.61	28.73
NS2	4.31	27.94	42.75	25.22	19.55	27.94
NS3	4.53	26.52	43.76	24.14	18.58	26.52
NS4	4.24	28.28	42.23	26.97	18.43	28.28

the proportion of holes decreases with increasing Na_2SO_4 solution concentration, reaching a minimum in sample NS4. This indicates that the Na_2SO_4 solution environment changes the pore distribution of the CMK cement soil, accounting for the change in porosity, and ultimately leading to a difference in strength.

Conclusions

In this study, CMK was used as a cement-soil additive, and its strength characteristics in an Na_2SO_4 solution environment were determined. The Na_2SO_4 solution concentration was varied to determine the influence of the Na_2SO_4 solution concentration on the compressive strength of CMK cement soil. Based on the laboratory results, the following conclusions could be drawn:

(1) The compressive strength of the CMK cement soil cured in different concentrations of Na_2SO_4 solution differed. When the Na_2SO_4 solution concentration was 18 g/L, the compressive strength of the CMK cement soil reached its maximum value.

(2) In the Na_2SO_4 solution environment, the albite generated by the reaction contributed to the ion-exchange reaction owing to the presence of Na^+, making the soil particle structure unit of the CMK cement soil more compact and increasing its strength.

(3) In the Na_2SO_4 solution environment, ettringite generated by the reaction had a dual effect. When the Na_2SO_4 solution concentration was appropriate, the ettringite had certain filling and expansion effects on the CMK cement soil due to the presence of SO_4^{2-}.

(4) The Na_2SO_4 solution changed the pore distribution in the CMK cement soil, leading to a change in its porosity, causing a change in its strength.

Acknowledgments

Conflict of Interest

The authors declare no conflict of interest.

References

1. TRAN K.Q., SATOMI T., TAKAHASHI H. Improvement of mechanical behavior of cemented soil reinforced with waste cornsilk fibers. Construction and Building Materials, **178**, 204, **2018**.

2. XU F., WEI H., QIAN W.X., CAI Y.B. Composite alkaline activator on cemented soil: Multiple tests and mechanism analyses. Construction and Building Materials, **188**, 433, **2018**.

3. SHAHRAM P., AFSHIN A., BUJANG B.K.H., MOHAMMAD, H.F. Stabilization of clayey soil using ultrafine palm oil fuel ash (POFA) and cement. Transportation Geotechnics, **3**, 24, **2015**.

4. MENGER E.D.S., BENETTI M., FESTUGATO L., IBEIRO L.D.S., LUZA R.D. Hydraulic conductivity and compressive strength of cemented soils. Geotechnical and Geological Engineering, **38** (6), 6031, **2020**.

5. CARO S., AGUDELO J.P., CAICEDO B., OROZCO L.F., PATIÑO F., RODADO N. Advanced characterisation of cement-stabilised lateritic soils to be used as road materials. International Journal of Pavement Engineering, **20** (12), 1425, **2018**.

6. SUGANYA K., SIVAPULLAIAH P.V. Compressibility of remoulded and cement-treated Kuttanad soil. Soils and Foundations, **60** (3), 697, **2020**.

7. MAK M.S.H., RAO P., LO I.M.C. Effects of hardness and alkalinity on the removal of arsenic(V) from humic acid-deficient and humic acid-rich groundwater by zero-valent iron. Water Research, **43** (17), 4296, **2009**.

8. LILLICRAP A.M., BIERMANN V., GEORGE R.J., GRAY D.J., OLDHAM C.E. The distribution and origins of extremely acidic saline groundwaters in the south of Western Australia - Groundwater and digital mapping datasets provide new insights. Journal of Hydrology, **556**, 717, **2018**.

9. SATYANARAYANA REDDY C.N.V., PRASAD A.C.S.V. Performance studies on cement stabilized gravelly soil exposed to sulfate environment. Indian Geotechnical Journal, **45** (2), 217, **2014**.

10. LIU S.Y., ZHENG X., CAI G.H., CAO J.J. Study of resistance to sulfate attack of carbonated reactive MgO-stabilized soils. Rock and Soil Mechanics, **37** (11), 3057, **2016**.

11. BAI X.H., ZHAO Y.Q., HAN P.J., QIAO J.Y., WU Z.A. Experimental study on mechanical property of cemented soil under environmental contaminations. Chinese Journal of Geotechnical Engineering, **29** (8), 1260, **2007**.

12. DONG X.Q., BAI X.H., LV Y.K. Study on the electrical resistivity and strength of cemented soil contaminated by sodium sulfate. China Civil Engineering Journal, **44** (A2), 186, **2011**.

13. LIU Q.S., QU J.W., LIU Z.P., HE J. Experimental study of mechanical properties of cemented soil under corrosion influence. Rock and Soil Mechanics, **35** (12), 3377, **2014**.

14. CHEN S.L., ZHANG J.Y., WEI X. Experimental study on dynamic elastic modulus of cemented soil in different environment. Journal of Vibration and Shock, **35** (18), 181, **2016**.

15. KAMPALA A., JITSANGIAM P., PIMRAKSA K., CHINDAPRASIRT P. An investigation of sulfate effects on compaction characteristics and strength development of cement-treated sulfate bearing clay subgrade. Road Materials and Pavement Design, **22** (10), 2396, **2021**.

16. SANCHEZ M.A., GARCIA H.L.C., MOLINA W.M, GUZMAN E.M.A., ACOSTA A.A.T., ORTEGA J.M.P. Use of metakaolin or coal gangue as a partial substitution of cement in mechanical performance of PC mortars. European Journal of Environmental and Civil Engineering, **25** (3), 502, **2021**.

17. SHAH V., PARASHAR A., SCOTT A. Understanding the importance of carbonates on the performance of Portland metakaolin cement. Construction and Building Materials, **319**, 126155, **2022**.

18. LIU J.P., LI X.Y., LU Y.S., BAI X.H. Effects of Na/Al ratio on mechanical properties and microstructure of red mud-coal metakaolin geopolymer. Construction and Building Materials, **263**, 120653, **2020**.

19. LIU J.P., CHEN W.M., XIE G.S., XIE X.Q., NING Q.J., BAI X.H. Strength characteristics and electrochemical impedance spectroscopy study of red mud-coal metakaolin geopolymer in a hydrochloric acid environment. International Journal of Electrochemical Science, **18** (7), 100182, **2023**.

20. MO Z.Y., GAO X.J. Research progress on the durability of metakaolin concrete. Materials Reports, **31** (15), 115, **2017**.

21. MO Z.Y., LIU Y.L., WANG D.W., LI Z.J., BAI L.G. Research progress on the physical properties of cement-based materials blended with metakaolin. Bulletin of the Chinese Ceramic Society, **37** (3), 911, **2018**.

22. ZHENG W.Z., ZOU M.N., WANG Y. Literature review of alkali-activated cementitious materials. Journal of Building Structures, **40** (1), 28, **2019**.

23. ASGHARI Y., MOHAMMADYAN Y.S.E., KOLOOR S.S.R. Utilization of metakaolin on the properties of self-consolidating concrete: A review. Construction and Building Materials, **389**, 131605, **2023**.

24. SIDDIQUE R., KLAUS J. Influence of metakaolin on the properties of mortar and concrete: A review. Applied Clay Science, **43** (3), 392, **2009**.

25. JANOTKA I., PUERTAS F., PALACIOS M., KULIFFAYOVÁ M., VARGA C. Metakaolin sand-blended-cement pastes: Rheology, hydration process and mechanical properties. Construction and Building Materials, **24** (5), 791, **2010**.

26. HASSAN A.A.A., LACHEMI M., AND HOSSAIN K.M.A. Effect of metakaolin and silica fume on the durability of self-consolidating concrete. Cement and Concrete Composites, **34** (6), 801, **2012**.

27. DENG Y.F., WU Z.L., LIU S.Y., YUE X.B., ZHU L.L., CHEN J.H., GUAN Y.F. Influence of geopolymer on strength of cement-stabilized soils and its mechanism. Chinese Journal of Geotechnical Engineering, **38** (3), 446, **2016**.

28. WANG S.N., GAO X.Q., WU Z.J., HUI H.L., ZHANG X.J. Permeability characteristics of cemented silty sand improved by metakaolin. Rock and Soil Mechanics, **43** (11), 3003, **2022**.

29. GB 50021-2001, Code for investigation of geotechnical engineering. China Architecture and Building Press: Beijing, China, **2009**.

30. WANG L.H., LI X.Y., CHENG Y., BAI X.H. Effects of coal-metakaolin on the properties of cemented sandy soil and its mechanisms. Construction and Building Materials, **166**, 592, **2018**.

31. WANG L.H., LI X.Y., CHENG Y., ZHANG Y.F., BAI X.H. Effects of coal-bearing metakaolin on the compressive strength and permeability of cemented silty soil and mechanisms. Construction and Building Materials, **186**, 174, **2018**.

32. MOBINA T.P.A., ASSKAR J.C., MOEIN G., SAMAN S.K. Investigation of the effect of the coal wastes on the mechanical properties of the cement-treated sandy soil. Construction and Building Materials, **239**, 117848, **2020**.

33. HAN P.J., LIU X., BAI X.H. Effect of sodium sulfate on strength and micropores of cemented soil. Rock and Soil Mechanics, **35** (9), 2555, **2014**.

34. GU J.X., ZENG C., LYU H.B., YANG J.Y. Effects of cement content and curing period on strength enhancement of cemented calcareous sand. Marine Georesources and Geotechnology, **39** (9), 1083, **2020**.

35. ISMAIL M. A., JOER H.A., SIM W.H., RANDOLPH, M.F. Effect of cement type on shear behavior of cemented calcareous soil. Journal of Geotechnical Engineering, **128** (6), 520, **2002**.

36. LIU S.Y., ZHANG D.W., LIU Z.B., DENG Y.F. Assessment of unconfined compressive strength of cement stabilized marine clay. Marine Georesources and Geotechnology, **26** (1), 19, **2008**.

37. YANG S., LIU W.B. Research on unconstrained compressive strength and microstructure of calcareous sand with curing agent. Journal of Marine Science and Engineering, **7** (9), 294, **2019**.

38. ZHAO H.H., ZHOU K., ZHAO C.J., GONG W.B., LIU J. A long term investigation on microstructure of cement-stabilized Handan clay. European Journal of Environmental and Civil Engineering, **20** (2), 1, **2015**.

39. HAN P.J., WANG S., CHEN F.Y., BAI X.H. Mechanism of cement-stabilized soil polluted by magnesium sulfate. Journal of Central South University, **22** (5), 1869, **2015**.

40. WANG Z.S., WANG D.X. Performance of industrial residue-cement solidified soils in resisting sulfate erosion. Chinese Journal of Geotechnical Engineering, **44** (11), 2035, **2021**.

41. HAN P.J., CHEN Y.F., SHEN B.Z., DU D.Y. Experimental investigation of the corrosion mechanism of cemented soils in magnesium sulfate solution. Materials Testing, **56** (9), 675, **2014**.

42. COLOMBO A., GEIKER M., JUSTNES H., LAUTEN R.A., DE WEERDT K. The effect of calcium

lignosulfonate on ettringite formation in cement paste. Cement and Concrete Research, **107**, 188, **2018**.

43. HOSSACK A.M., THOMAS M.D.A. The effect of temperature on the rate of sulfate attack of Portland cement blended mortars in Na_2SO_4 solution. Cement and Concrete Research, **73**, 136, **2015**.

44. CUI D.S., XIANG W. Pore diameter distribution test of red clay treated with ISS. Rock and Soil Mechanics, **31** (10), 3096, **2010**.

45. HAN P.J., ZHANG W.B., LIU X., BAI X.H. Early strength of cemented soils polluted by magnesium chloride. Chinese Journal of Geotechnical Engineering, **36** (6), 1173, **2014**.